

The May 1997 SOHO-Ulysses quadrature

S. T. Suess,¹ G. Poletto,² M. Romoli,³ M. Neugebauer,⁴ B. E. Goldstein,⁴
and G. Simnett⁵

Abstract. We present results from the May 1997 SOHO-Ulysses quadrature (SOHO-Sun-Ulysses angle=90°), near sunspot minimum. Ulysses was at 5.1 AU, 10° north of the solar equator, and off the east limb. It was also at the very northern edge of the streamer belt. Nevertheless, the Solar Wind Observations Over the Poles of the Sun instrument (SWOOPS) detected only slow, unusually smooth wind and there was no direct evidence of fast wind from the northern polar coronal hole or of mixing with fast wind. The Large-Angle and Spectrometric Coronagraph (LASCO) images show that the streamer belt at 10°N was narrow and sharp at the beginning and end of the 2 week observation interval, but broadened in the middle. A related change in density, but not flow speed, occurred at Ulysses. Under these conditions it was possible to show that densities derived from the Ultraviolet Coronagraph Spectrometer (UVCS) in the lower corona are closely related to those in the solar wind, both over quiet intervals and in transient events on the limb. Density and velocity in one small transient observed by both LASCO and UVCS are analyzed in detail.

1. Introduction

SOHO-Ulysses quadrature occurs when the SOHO-Sun-Ulysses included angle is 90°. At such times, plasma leaving the Sun in the direction of Ulysses can first be remotely observed by SOHO instruments and then later be sampled in situ by Ulysses instruments. It is the best time to make such a direct comparison. The quadratures occur twice a year as SOHO moves around the Sun. Figure 1 is a diagram of the orbits of SOHO and Ulysses which illustrates why quadratures occur. As shown, Ulysses is in a near polar solar orbit, inclined at 80° to the heliographic equator, with aphelion of 5.4 AU, perihelion of 1.34 AU, and period of about 5 years. The plane of the orbit is essentially fixed in the heliographic-inertial frame of reference. SOHO is at the L1 Lagrangian point between Earth and the Sun so it revolves with the Earth around the Sun once a year. The distance from Earth to SOHO is only 1% of the Earth-Sun distance, so SOHO and Earth are ef-

fectively at the same location for the purpose of making coordinated observations with Ulysses. Locations in the SOHO orbit at which quadrature occurs are indicated by triangles.

We report here on the May 1997 quadrature. SOHO was on the near side of the Sun in Figure 1, and a dashed line is drawn from the SOHO location to the east limb of the Sun at ~ 10° above the equator, the latitude of Ulysses, and then is continued at a right angle and goes directly to the location of Ulysses on the left portion of its orbit. This is the time when limb observations at the position angle of Ulysses can be used to analyze plasma which later reaches Ulysses. There are several measurements that could be made with instruments on SOHO and the results compared with the instruments on Ulysses. These include measurements of solar wind density, temperature, flow speed, magnetic field, composition, and transient behavior. We use data from the SOHO Large-Angle Spectrometric Coronagraph (LASCO) C2 white light coronagraph to define the morphology of the corona, the SOHO Ultraviolet Coronagraph Spectrometer (UVCS) to measure the density and flow speed (using the Doppler dimming technique [Kohl and Withbroe, 1982]) in and above the streamer, and the Ulysses Solar Wind Observations Over the Poles of the Sun instrument (SWOOPS) for the resulting solar wind density, speed, and temperature. Data from the Ulysses vector helium and flux gate magnetometers (VHM/FGM) are used to assess the state of the interplanetary magnetic field (IMF).

The data were taken near solar minimum, in the streamer belt (at the Sun) or in slow solar wind (at Ulysses). Therefore the emphasis on the analysis will

¹NASA Marshall Space Flight Center, Huntsville, Alabama.

²Osservatorio Astrofisico di Arcetri, Firenze, Italy.

³Department of Astronomy, Università di Firenze, Firenze, Italy.

⁴Jet Propulsion Laboratory, California Institute of Technology, Pasadena.

⁵School of Physics and Astronomy, University of Birmingham, Birmingham, England.

Copyright 2000 by the American Geophysical Union.

Paper number 2000JA000044.
0148-0227/00/2000JA000044\$09.00

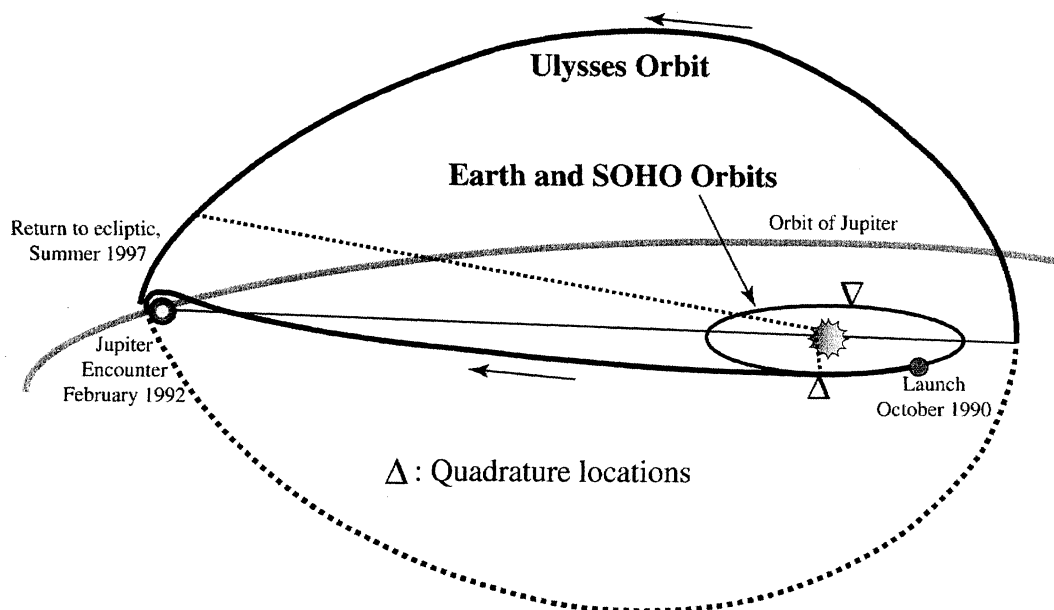


Figure 1. Orbits of Ulysses and SOHO/Earth. SOHO orbits the Sun with the Earth so no distinction is made between the two. Ulysses' orbit is inclined to the heliographic equator by 80° , has an aphelion of 5.4 AU, a perihelion of 1.34 AU, and is essentially stationary with respect to the Sun. Since it takes the Earth and SOHO 1 year to circumnavigate the Sun, the included angle between Ulysses and SOHO, as measured with respect to the Sun, is generally 90° twice a year. The locations where this occurs in the SOHO orbit are marked here with triangles and these times are when Ulysses and SOHO are in quadrature. The May 1997 quadrature observations are indicated with dashed lines. SOHO was on the near side of the Sun, at the upward pointing triangle, observing 10° north of the equator off the east limb. Ulysses was at 5.1 AU, 10° north of the equator, also off the east limb.

be on flow properties of slow solar wind. This opportunity was an unusually good chance to analyze the slow solar wind since the Sun exhibited near solar minimum conditions at the same time as there was an absence of high-speed streams and obvious concomitant corotating interaction region (CIR) effects at Ulysses. This is illustrated in Figure 2, which shows both the smoothed Boulder daily sunspot number for the 10 year period ending just after the May 1997 quadrature and the solar wind speed at Ulysses from October 1996 through September 1997. The sunspot number had just begun to rise in May 1997, so observations made at successive quadratures would have missed solar minimum conditions. At the same time, Ulysses was deep in a series of CIRs, caused by an equatorial extension of the north polar coronal hole, up until the solar rotation preceding the May 1997 quadrature. *McComas et al.* [1998] described this more fully, showing that Ulysses was seeing corotating high-speed streams of the same magnetic polarity as the north polar coronal hole up until the beginning of May 1997. The CIRs disappeared just at that time, when Ulysses became completely immersed in the slow wind coming from the equatorial streamer belt. For these reasons, it would have been impossible to assess unmodified slow solar wind at an earlier quadrature. The May 1997 quadrature presents a unique opportunity to analyze slow wind at solar minimum.

The Ulysses-Sun-SOHO angle (Θ) changes by $\sim 1^\circ$ per day, or just the orbital motion of SOHO about the Sun, while the uncertainty in the location on the Sun from which solar wind originates, as determined by extrapolating backward from Ulysses, is no less than $\pm 5^\circ$, due both to nonradial flows in the corona and to inaccuracies in assumptions made in the extrapolation. Because of this, we make observations for several days on either side of quadrature, over which Θ changes by less than the extrapolation uncertainty. In addition, by making limb observations over an extended period, the extrapolation uncertainty can be reduced through matching changes in flow at Ulysses with morphological changes at the Sun. This approach works best if solar features are changing slowly as they rotate past the limb. It also works on the occasion of large transients which can easily be correlated with subsequent changes at Ulysses. In the present case the former conditions prevailed. The occurrence of quadratures is independent of solar rotation, but the sidereal solar rotation period's being 25.5 days means that observations for the 2 weeks centered on quadrature can be used to study solar wind coming from a longitudinal swath of up to $\sim 180^\circ$ on the Sun (as the Sun rotates beneath the foot point of Ulysses).

For the May 1997 quadrature we selected the 12 day interval May 21 to 1 June during which Θ ranged be-

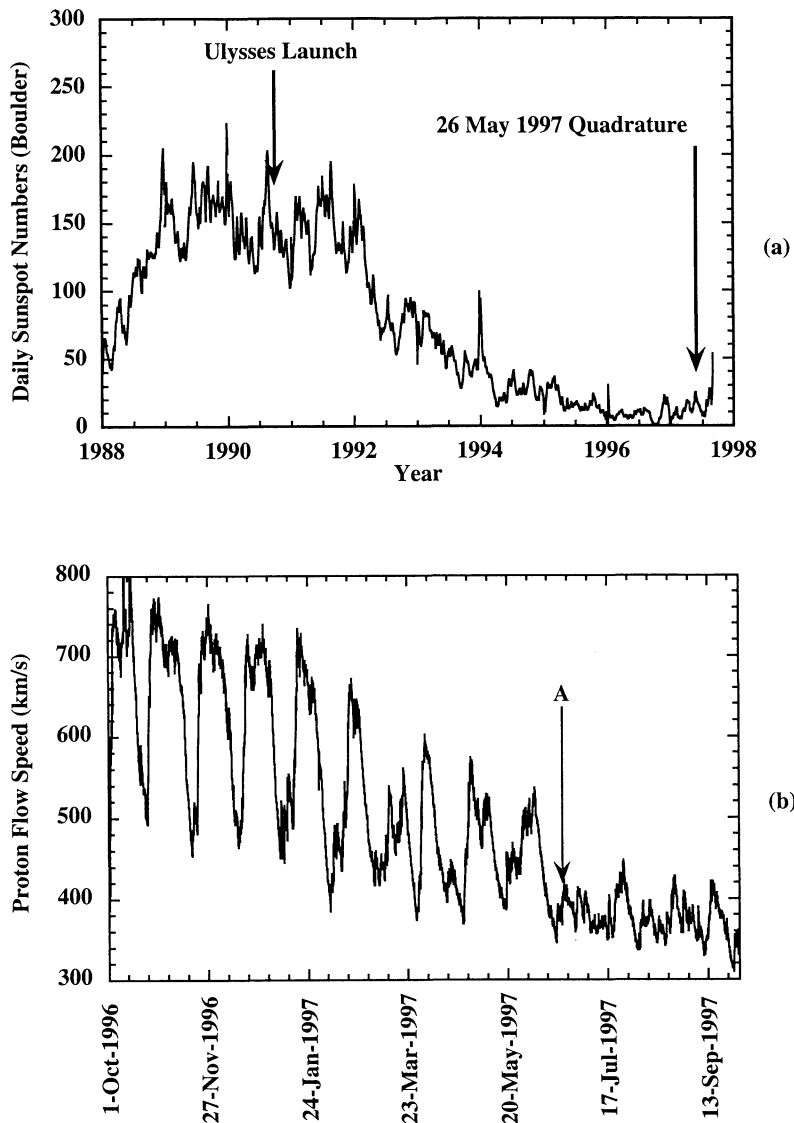


Figure 2. (a) Solar daily sunspot number (Boulder/Space Environment Center) showing that while Ulysses was launched near sunspot maximum, the May 1997 quadrature occurred very near sunspot minimum. (b) Solar wind speed variation at Ulysses showing the predominance of corotating interaction regions from equatorial extensions of coronal holes up until the time of the quadrature, marked here by “A”.

tween $\sim 85^\circ$ and $\sim 107^\circ$ and over which the Sun rotated through an angle of about 160° . The rotation of the Sun, combined with near solar minimum conditions at the time of the observations, means that the primary changes imposed on the solar wind reaching Ulysses were due to the rotation of relatively simple streamers past the limb of the Sun rather than to coronal transients.

In section 2.1 we present LASCO C2 results, setting the context for the solar wind observations. In section 2.2 we show the Ulysses/SWOOPS in situ data and extrapolate them back to the Sun. In section 2.3 we compare the behavior of densities and flow speeds at low heliocentric heights, as inferred from UVCS observations, with the behavior of the same parameters

inferred from in situ observations. A subject which we specifically address is the relationship between temporal variations in UVCS data, temporal variations in C2 white light data, and temporal variations at Ulysses. These three sections give sufficient results for a general discussion of the observations in section 2.4. We then turn to more detailed aspects of the data. In section 3 the large transients seen in LASCO C2 are discussed and compared with SWOOPS and VHM/FGM data to see if any of these transients had identifiable consequences in the plasma and magnetic field parameters at Ulysses. We will show that no such effects were seen. In section 4 we analyze a small UVCS transient seen on May 26 that may have had a signature in the Ulysses data. section 5 summarizes the results from analyzing

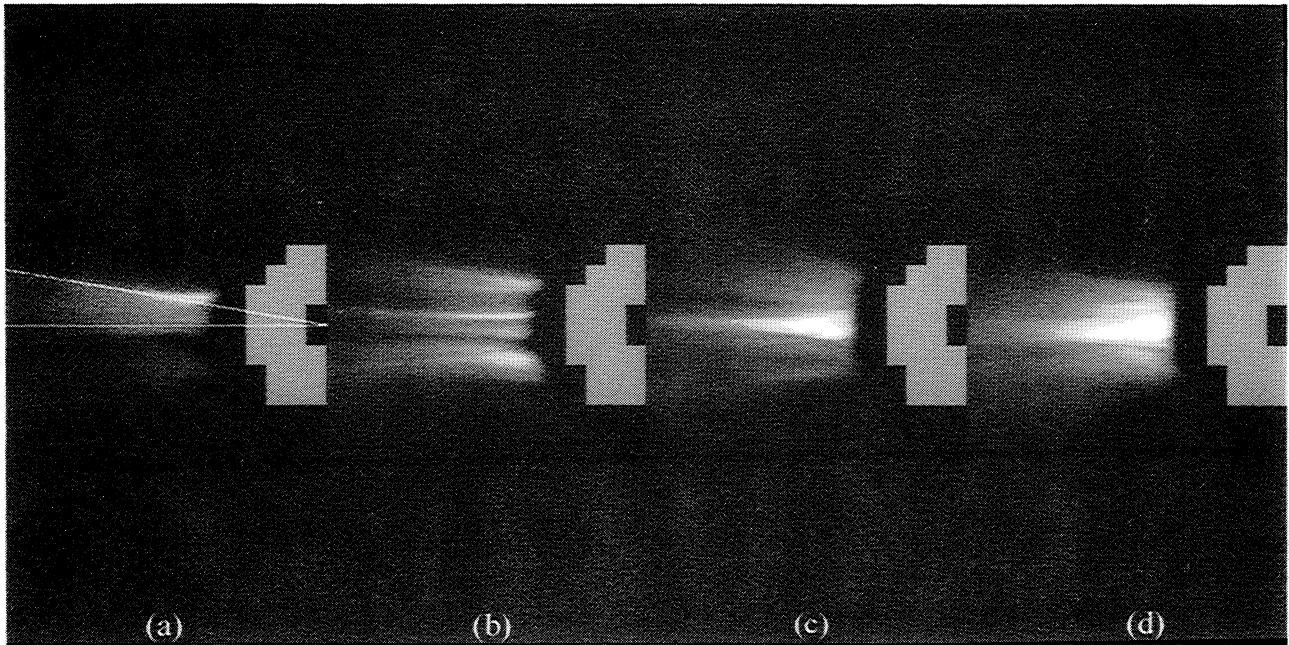


Figure 3. LASCO/C2 images from (a) May 22, (b) May 26, (c) May 29, and (d) June 1, 1997. The white line shows the direction to Ulysses. The streamer belt was confined to the equator during this entire interval, but changed appearance. There was a bright, isolated streamer during May 21–25 and also from May 29 to June 1. During May 26–28, the equatorial streamer broadened into a fan (or “forest”) made up of several rays without an obvious isolated streamer.

slow solar wind by comparing observations made at the Sun with SOHO and observations made in the solar wind with Ulysses during the May 1997 SOHO-Ulysses quadrature.

2. LASCO C2, SWOOPS, and UVCS Observations

2.1. LASCO C2

Figure 3 shows LASCO C2 direct and unpolarized white light coronagraph images [Brueckner et al., 1995] taken on May 22 at 1030, May 26 at 1030, May 29 at 1634, and June 1, 1997 at 2230 (Figures 3a, 3b, 3c, and 3d, respectively). The direction to Ulysses is shown by the white line 10° north of the white line at the equator on the east limb in Figure 3a. It can be seen that on May 22 and June 1 Ulysses lay at the northern edge of the bright streamer.

During the entire period of May 21 to June 1, 1997, the east limb of the Sun was dominated by streamers at the equator and large coronal holes over both poles. However, as the Sun rotated, the character of the equatorial streamers changed. At the beginning (Figure 3a) the streamer was somewhat diffuse, but was made up of a single structure with a very sharp edge at the north. Over May 23–24, the streamer changed into a fan of bright rays that persisted for several days, although the individual rays came and went. This suggested a “forest” of quasi-steady bright rays was being swept past

the limb of the Sun by solar rotation. On May 29, the east limb equatorial streamer returned to a single but even more narrow structure than existed on May 22. The north edge of that streamer was less sharp than on May 21, but was still poleward of the latitude of Ulysses.

LASCO makes ~ 50 C2 images each day and mpeg movies are readily available from the LASCO web site (http://lasco-www.nrl.navy.mil/daily_mpg/), made at a cadence of approximately one each $1/2$ hour. We surveyed images and mpeg movies for coronal mass ejections (CMEs), and each day during the observing interval was classified as to whether it was quiet or contained a CME. Quiet days were further distinguished between those with apparent evolutionary or transient changes in the east limb streamers and those in which the streamer was apparently steady. The results are summarized in Table 1. Small CMEs were found on the east limb on May 23, May 25, and June 1. Later we will discuss whether these CMEs might have been on or off the limb, and whether they affected the solar wind at Ulysses. Generally, however, conditions at both Ulysses and the Sun were unusually quiet throughout the entire 12 day interval.

The most obvious change seen in the LASCO images is the fanning out of the east limb streamer on May 24–29. The reason this happened can be seen from the Wilcox Solar Observatory photospheric and source surface magnetic fields for Carrington Rotation 1923 (CR

Table 1. East Limb Phenomena From LASCO-C2

Date	Quiet?	Notes
May 19	no	CME 0130-2400. Single isolated streamer, bright north edge.
May 20	yes	Single isolated streamer, bright north edge.
May 21	yes	Single isolated streamer, bright north edge.
May 22	(yes)	Swelling in base of streamer at 2300, in southern quadrant. Streamer unaffected. Single isolated streamer, bright north edge.
May 23	no	Small CME 0000-1100, quiet rest of the day. Streamer is unaffected.
May 24	yes	Streamer slowly becomes broader and more diffuse on northern edge, with more rays.
May 25	no	Small CME 1500-1900. Streamer is broader, with more rays, at end of day.
May 26	(yes)	Small changes at start and end of the day (0100-0430, 1930-2400). Slow evolution throughout the day.
May 27	(yes)	Slow evolution throughout the day.
May 28	yes	Streamer is still broadened into a forest.
May 29	(yes)	Small fluctuations on northern edge. North edge has faded or withdrawn equatorward by end of day, leaving a sharp streamer.
May 30	yes	Narrow, sharp streamer, diffuse north edge.
May 31	yes	Narrow, sharp streamer, diffuse north edge.
June 1	no	Small CME 0800-1700. The streamer is not visibly affected.

Parentetical “(yes)” denotes less than perfectly quiet.

1923) that are shown in Figures 4 and 5. In Figure 5 a shaded box is drawn around the longitude range 200° - 250° , corresponding to the time-shifted interval of the forest of bright rays that is shown in Figure 3b. A north-south positive unipolar region is at $\sim 210^\circ$, and a north-south negative region is at $\sim 230^\circ$. This suggests an arcade that was highly inclined away from the equator as the explanation for the forest. The resulting source surface neutral line in Figure 4 shows that the heliospheric current sheet (HCS) was predicted to have a dislocation due to the north-south unipolar regions in the photosphere. The May 24-29 fanning out of the streamer closely corresponds to conditions during the LASCO C2 observations reported by Wang *et al.* [1997] for data taken in 1996. They similarly reported a dislocation in the neutral line and an inferred tilt in the streamer belt. It appears that conditions then were almost identical to those during May-June 1997 and we adopt their interpretation for the fanning out of the streamer belt on May 24-29.

2.2. SWOOPS

The Ulysses solar wind plasma instrument measures the three-dimensional ion and electron velocity distributions every 4 or 8 min. Here we use 1 hour average data for protons: the speed, number density, and temperature. We also use supplemental data from VHM/FGM, the Ulysses vector magnetometer.

In May-June 1997, Ulysses was 5.1 AU from the Sun, the solar wind speed was $375 \pm 25 \text{ km s}^{-1}$, and it took about 3 weeks for solar wind plasma to pass from the Sun to Ulysses. $\Theta = 90^\circ$ occurred on May 26, so the corresponding date the solar wind reached Ulysses was around June 16. The 12 day interval May 21 to June 1 for SOHO observations therefore roughly corresponded to June 11 to June 23 at Ulysses. This serves for estimating when to examine Ulysses data. Over the 12 day interval, Ulysses moved $< 1^\circ$ in latitude and so can be considered to have also been at a fixed solar latitude during this time. The source time for the solar wind at Ulysses is found by extrapolating back to the Sun using the measured speed and the distance, latitude, and longitude of Ulysses. We used the constant velocity approximation (CVA) to extrapolate the solar wind back to one solar radius. This type of extrapolation is generally uncertain to no better than $\sim \pm 5^\circ$, but we have direct observations of the solar corona which allow us to confirm the extrapolation by comparison with variations in the structure of the corona and to make adjustments if there are discrepancies. As will be seen, the remarkable conditions in May-June 1997 allow the extrapolation to be remarkably accurate. Specifically, the nearly constant radial flow speed meant there was little dynamic interaction and enabled a more accurate extrapolation using the CVA.

Two competing processes partially counteract each other to further increase the accuracy of the CVA. Corotation of solar wind plasma with the Sun is significant out to the Alfvén radius [Weber and Davis, 1967], shifting the extrapolated CVA departure longitude at the Sun eastward. Conversely, the solar wind speed decreases near the Sun, shifting the extrapolated CVA departure longitude westward. Both effects are of the same order of magnitude, a few degrees.

Figure 6a shows the 1 hour average solar wind data from June 14 to 29, 1997 (day of year (DoY) 165-180) at Ulysses. The speed is between ~ 350 and 425 km s^{-1} throughout the interval, with relatively small variability except for a small shock jump of 35 km/s on day 168. For comparison, Figure 6b shows flow speed for 2 weeks in the summer of 1997 when Ulysses was still close to the heliographic equator and at 5.1 AU, but immersed in typical slow solar wind. The variability was 31% larger than in June and similar to typical slow wind observed at other distances and latitudes [Phillips *et al.*, 1995]. There were also at least two shocks (see arrows in Figure 6b) similar to the small shock seen at

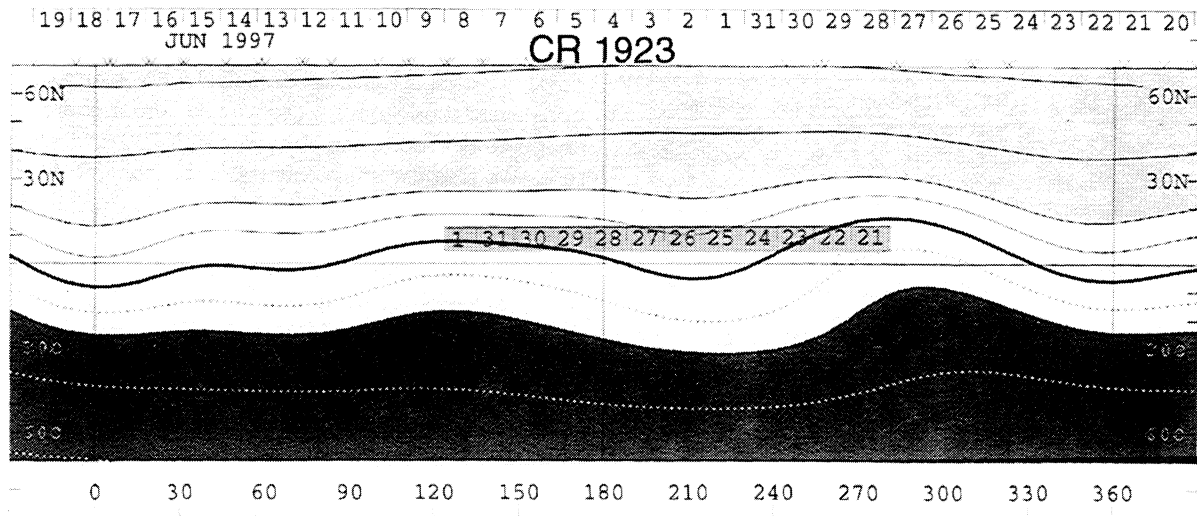


Figure 4. Source surface magnetic field map from Wilcox Solar Observatory (Solar-Geophysical Data, 636(1), 1997) for Carrington rotation 1923, showing data from May 20 through June 19, 1997. The contour levels are 0 and plus or minus 1, 2, 5, 10, and 20 mT. The horizontal scale at the bottom is heliographic longitude. The neutral line is shown as the heavy solid, wavy line near the equator and this line is commonly used to predict the center of the streamer belt. A shaded band has been superimposed on the map, centered on the latitude of Ulysses and showing the location of the limb on the indicated dates in May 1997. This band is the source location for wind later detected at Ulysses.

quadrature. This illustrates that the solar wind in June 1997 was unusually quiet and that the shock was not atypical.

The density and magnetic field in Figure 6a show a higher variability after the shock. In addition, two features are particularly noticeable. First, the shaded

region is a time of low ion plasma β (≤ 0.5) such as is often found in CMEs. At the same time, there was an anomalously low helium abundance of $\sim 1\%$ which is less common but not unknown in CMEs. This interval and the CMEs will be discussed in section 3. Second, there is a density spike at DoY 171.5 during which there

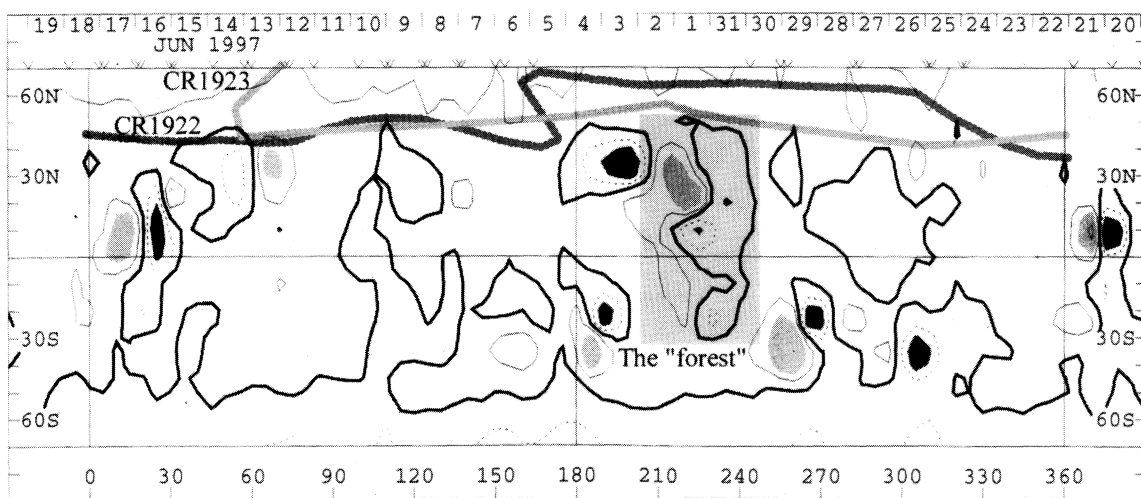


Figure 5. Photospheric line-of-sight magnetic field map from Wilcox Solar Observatory (Solar-Geophysical Data, 636(1), 1997) for Carrington rotation 1923, showing data from May 20 through June 19, 1997. The contour levels are 0 and plus or minus 100, 500, 1000, and 2000 mT. The region marked as the "forest" lies beneath the fanned out portion of the streamer belt noted in Figure 3b. The boundaries of the northern polar coronal hole for Carrington rotations 1922 and 1923 are marked in dark and light gray, respectively.

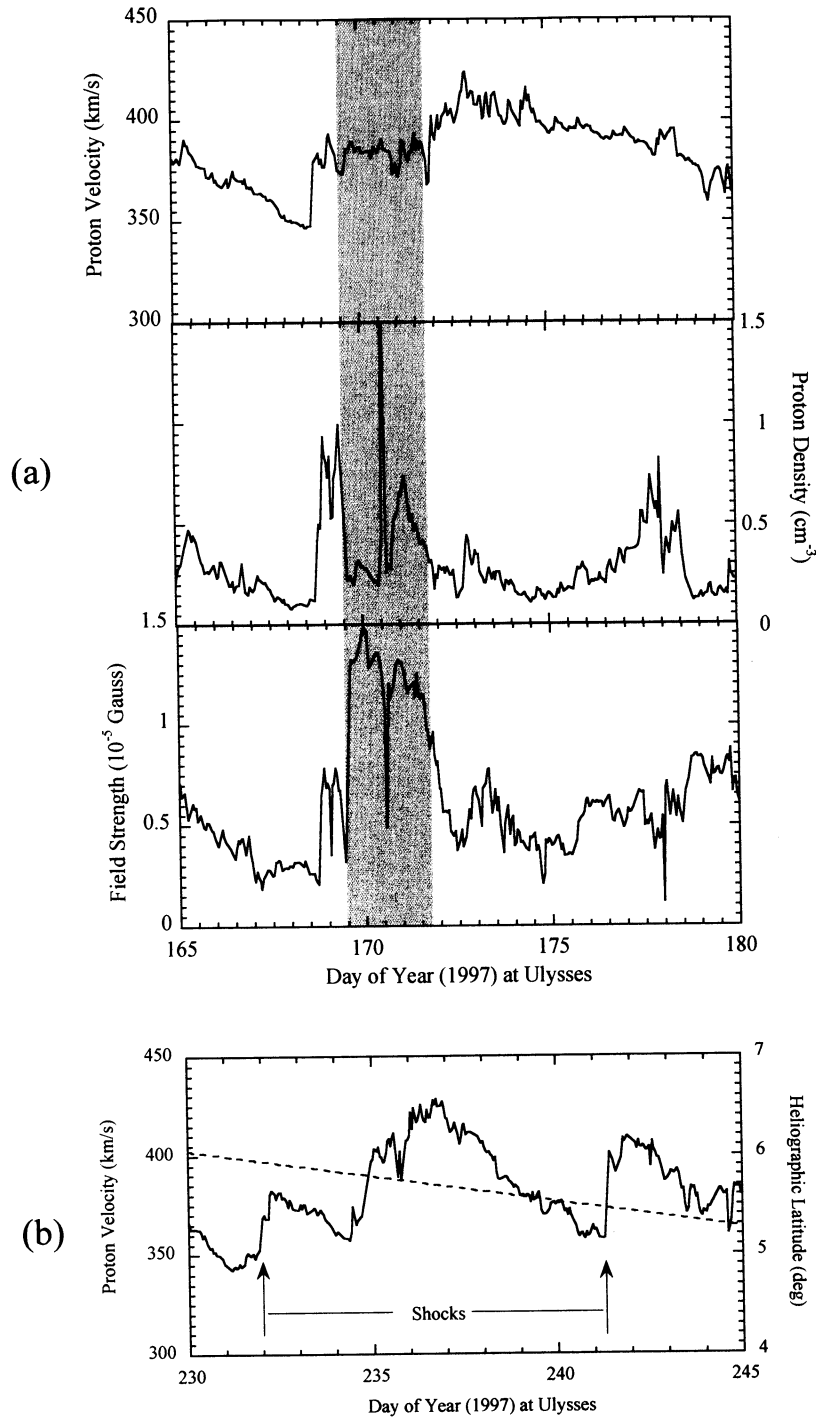


Figure 6. (a) One hour average values of the solar wind speed, proton number density, and magnetic field strength at Ulysses from June 14 to June 29, 1997 (DoY 165-180). (b) Solar wind speed (solid) from later in 1997 when Ulysses was still close to the heliographic equator and 5 AU but immersed in typical slow solar wind. The heliographic latitude of Ulysses is shown by the dashed line. Small shocks on DoY 232 and 241 are marked with arrows.

is a corresponding drop in field strength. This small, isolated, partially pressure-balanced structure will be discussed in section 4.

Figure 7 shows the solar wind speed and density from the quadrature interval after it has been mapped back

to the Sun. In this plot, the horizontal axis is the day of year the plasma left the Sun, where DoY 141 is May 21, 1997, and DoY 152 is June 1, 1997. To find the corresponding Carrington longitude, reference can be made to the scale shown in Figure 4, where it is seen

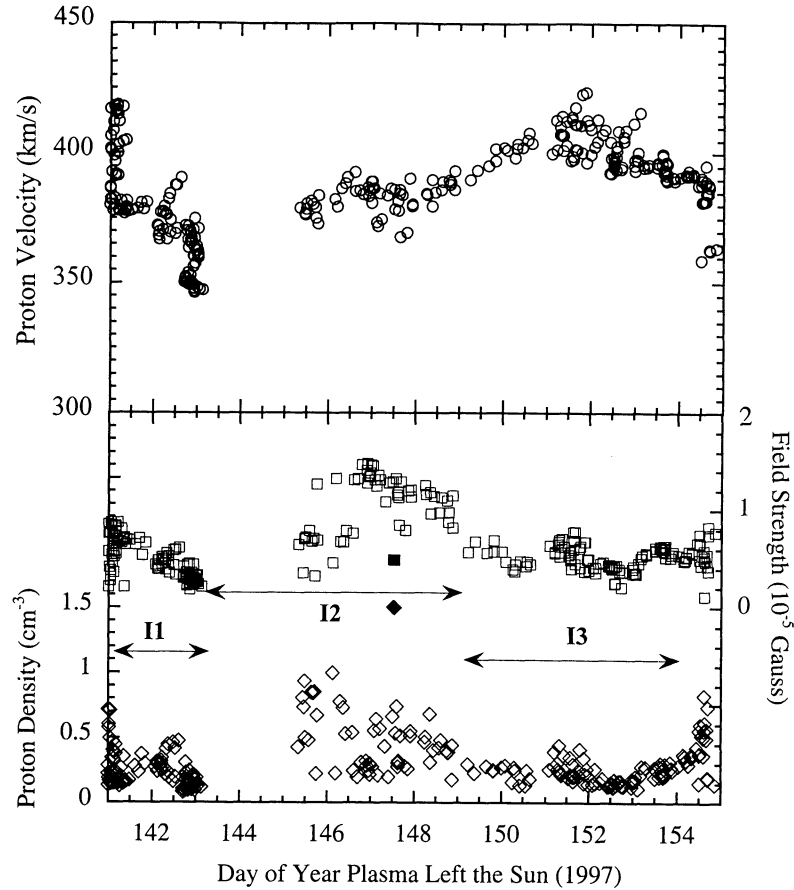


Figure 7. Solar wind speed, magnetic field strength, and density from the observing interval shown in Figure 6a, which has been mapped back to the Sun using the constant velocity approximation. The horizontal axis shows time in terms of the day the solar wind left the Sun. DoY 141 is May 21, 1997 and DoY 154 is June 3, 1997. Figure 4 can be used to convert DoY the wind left the Sun into Carrington longitude. The three intervals, I1, I2, and I3, and the two solid data points in field strength and density are discussed in the text.

that the extrapolated departure longitude ranges from $\sim 270^\circ$ - 280° on May 21 to $\sim 120^\circ$ - 130° on June 1. The gap between \sim DoY 143.5 and 145 in this Figure 7 is due to the shock; the faster plasma to the right of the shock in Figure 6 is extrapolated to leave the Sun at a later date.

The density data in Figure 7 fall naturally into three intervals; I1 from DoY 141.0 to 143.0, I2 from DoY 143.0 to 149.0, and I3 from DoY 149.0 to 151.0. Intervals I1 and I3 have low density variability in comparison to I2. These intervals closely correspond to the changing appearance of the streamer belt shown in Figure 3; intervals I1 and I3 are when there was one well-defined streamer, while interval I2 was when the streamer belt had fanned out into the forest. The solar wind proton and alpha particle temperatures behaved much the same way as the density, and these are shown in Figure 8. What imposed the density and temperature irregularities at the Sun may also have had corresponding fluctuations in flow speed, but such fluctuations would have had a scale size comparable to the density and

temperature signatures. It can easily be shown that such small-scale speed fluctuations will be eliminated by dynamical interactions far inside 5 AU [Neugebauer *et al.*, 1995], and this is probably why they were absent at Ulysses.

2.3. UVCS

During the SOHO-Ulysses quadrature, UVCS observed coronal plasma for about 9 hours per day. Observations were performed at 3.5 and 4.5 R_{SUN} , starting with an 8100 s observation at 3.5 R_{SUN} , followed by an equally long observation at 4.5 R_{SUN} . Subsequent observations alternated between the two heights, spending, as a rule, 2700 s at 3.5 R_{SUN} and 5400 s at 4.5 R_{SUN} . These exposure times are long enough to guarantee a high statistical significance of Lyman α data, because even at these altitudes, the line is fairly strong. The much weaker OVI lines are affected by statistical errors which may be fairly large (see section 4). Data have a spatial resolution of 21 arcsec per pixel:

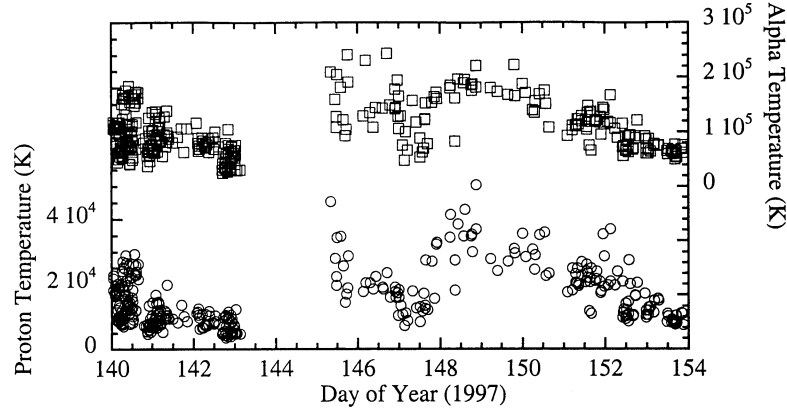


Figure 8. Proton and alpha particle temperatures from the observing interval shown in Figure 6a, mapped back to the Sun using the constant velocity approximation. The horizontal axis is the same as in Figure 7.

An average value over four (five) pixels has been considered representative of the line intensity over an $\approx 1^\circ$ latitude interval centered at $\approx 10^\circ$ latitude, at 3.5 (4.5) R_{SUN} . Data have been calibrated and corrected for flat field effects in the standard way [Gardner *et al.*, 1996]; no stray light correction has been applied because the stray light, at these heights, amounts to $\approx 10^{-9}$ of the disk intensity of the line (L. D. Gardner, private com-

munication, 1999) and its contribution to the total line intensity is negligible.

Analysis of UVCS data allows us to derive the temporal profile of two parameters that are also measured in situ, by Ulysses experiments: electron density (N_e) and flow speed. For an estimate of density variation, we can use the Ly α intensity, $I_{Ly \alpha}$, versus time because $I_{Ly \alpha}$ depends on density, electron temperature and flow

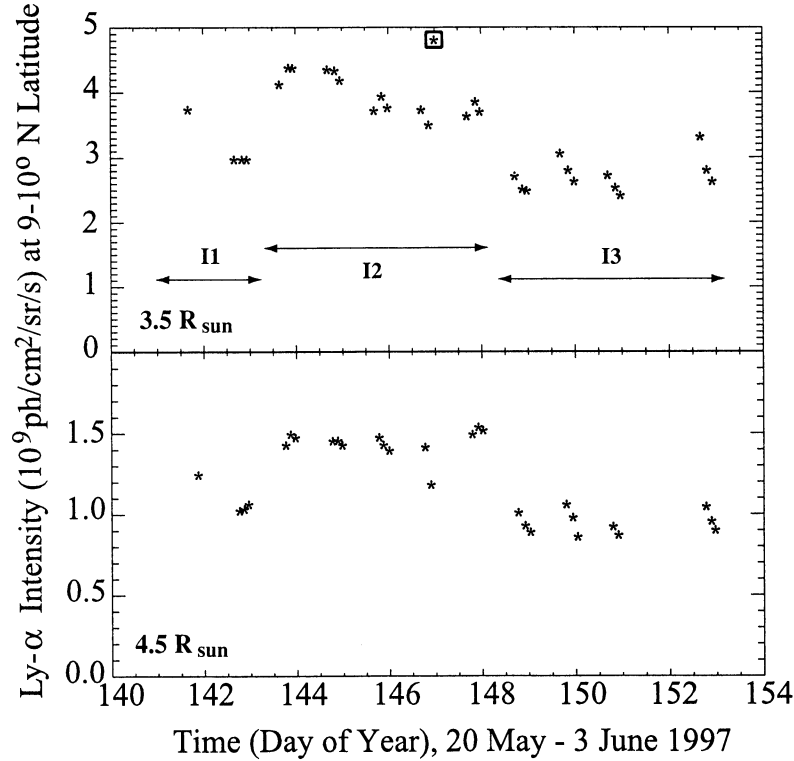


Figure 9. Ultraviolet Coronagraph Spectrometer (UVCS) Ly α intensity from DoY 141-153, in the $9^\circ - 10^\circ$ latitude range, during the May 1997 SOHO-Ulysses quadrature: (top) $I_{Ly \alpha}$ at $3.5 R_{SUN}$; (bottom) $I_{Ly \alpha}$ at $4.5 R_{SUN}$. Values have been averaged over the observing interval; the 1σ error bar is too small to show up on the scale of this figure. The intervals marked I1, I2, and I3 and the boxed data point in the top panel are described in the text.

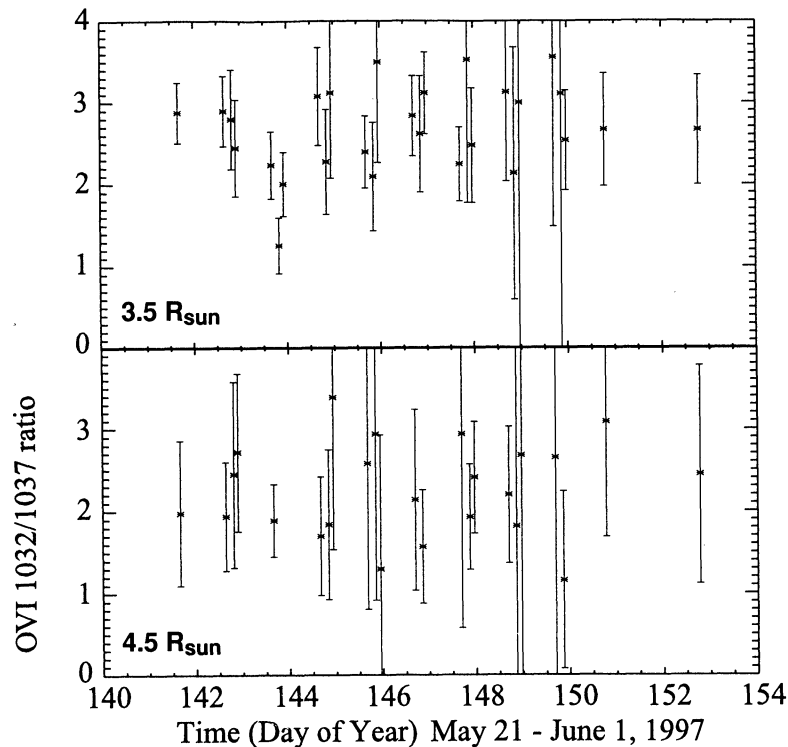


Figure 10. UVCS OVI 1032/1037 Å line ratio at (top) 3.5 and (bottom) 4.5 R_{SUN} , in the $9^\circ - 10^\circ$ latitude range, from DoY 141 to 153; the 1σ error bars are also shown.

speed (and, obviously, on spectroscopic parameters; see, for example, *Withbroe et al.* [1982]). Because major variations in electron temperatures are unlikely and the flow speed, in streamers, should not sensibly dim the $Ly\ \alpha$ intensity (flow speeds of about 75 km s^{-1} weaken the line by only 20%, via Doppler dimming effects), any fluctuation of $I_{Ly\ \alpha}$ is mainly due to density variations. Absolute values of the density at lower temporal resolution can be derived from the collisional component of the intensity of the OVI 1037 Å line, $I_{\text{OVI}37,\text{coll}}$ [*Corti et al.*, 1997]: This technique to infer densities from $I_{\text{OVI}37,\text{coll}}$ will be reviewed in section 4. Here, we focus on the plasma fluctuations. Absolute values of plasma parameters are not needed.

Analogously, variations in plasma flow speed, if any, within streamers may be inferred by studying the temporal variation of the ratio $R = I_{\text{OVI}32}/I_{\text{OVI}37}$ as a flow speed proxy. R depends on the flow speed because the Doppler dimming of the two lines is not the same [e.g., *Noci et al.*, 1987]; however, quantitative values of the flow speed can be derived only through modeling [e.g., *Cranmer et al.*, 1999] because of the complicated dependence of R on other plasma parameters as well (see Figure 16). Order-of-magnitude estimates of the plasma flow speed during an unusual event will be made in section 4.

Figure 9 shows the temporal profile of $I_{Ly\ \alpha}$ versus time from DoY 141 to DoY 153, to be compared with the SWOOPS densities: Every data point rep-

resents the average intensity over the observing time span. $I_{Ly\ \alpha}$ changes, over the quadrature interval, by less than a factor of 2, but there are definite subintervals that are distinct from each other and which correspond closely to the intervals I1, I2, and I3 of Figure 7 and are given again here. Obviously, the density pattern at 5 AU is analogous to the density pattern in the low corona. From this single example we cannot draw a general conclusion, but it is interesting to see that the correspondence is also maintained in the special case discussed in section 4.

The uncertainty in $I_{Ly-\alpha}$ is $< 5\%$ and therefore is not displayed in Figure 9. There is one data point at 3.5 R_{SUN} that does not follow the overall trend, the unusually high intensity/density observed late on DoY 146 (boxed data point). The high density value observed by SWOOPS on DoY 147.5 (Figure 7) may have been related (Figure 7, solid data points). This UVCS event is further discussed in section 4.

Figure 10 gives the temporal profile of R at 3.5 and 4.5 R_{SUN} . As in the $I_{Ly\ \alpha}$ plot, every data point represents the average of R over the observing interval. Count rates in OVI lines are so low, at these altitudes, that R is affected by large errors (see the 1σ error bars in the figure). As a consequence, no definite conclusion can be drawn from our observations other than data are not inconsistent with R being constant with time, as implied by Ulysses flow speed observations. Possibly, we can say that at 3.5 R_{SUN} , $R \approx 2.6$ (except on May

23) while, at $4.5 R_{\text{SUN}}$, $R \approx 2.0$. This may be an indication that OVI ions accelerate, in the altitude interval between $3.5 R_{\text{SUN}}$ and $4.5 R_{\text{SUN}}$. As we mentioned, knowledge of plasma temperatures (electron, and kinetic ion parallel and perpendicular temperatures) and densities is necessary to give a quantitative estimate of the plasma flow speed, and an attempt in this direction is made in section 4. However, we notice that a value of $R = 2.5$ is consistent with nearly all the data points at $4.5 R_{\text{SUN}}$; thus an alternative interpretation is that very little acceleration takes place in between the two heights, apart from sporadic cases.

Some more insight into this issue can be drawn if we give up on temporal resolution, sum over data acquired throughout each day, and consider the maximum deviation of the daily R values, with respect to their average over the whole observing interval, as an indication of the temporal fluctuations that can possibly be present. Then, at $3.5 R_{\text{SUN}}$ we have a deviation of $+15\%/-30\%$, and at $4.5 R_{\text{SUN}}$ we have a deviation of $+35\%/-20\%$. These figures, provided all the other parameters on which R depends are known and keep constant, may be translated into coronal flow speed excursions. Very crudely, we can say that in the low speed flow regime we are considering at present, if we ascribe changes in R uniquely to changes in flow speed, the variation in this parameter will be $\leq 30 - 35\%$. For a comparison, the highest excursions that are observed over the same time interval at Ulysses are $+12\%/-9\%$. This is consistent with the UVCS observations because we expect the excursion at Ulysses to be smaller than in the corona due to dynamic interactions.

There is one data point that does not follow the general trend: At $3.5 R_{\text{SUN}}$ a low R value has been derived on DoY 143. This is not mimicked by high-speed values in in situ observations. If it was a transient only in speed, then such a brief speed fluctuation would never survive to 5 AU [Neugebauer *et al.*, 1995]. There was no corresponding fluctuation in $I_{\text{Ly } \alpha}$.

2.4. Synopsis

The solar wind at Ulysses was not just slow during the May 1997 quadrature; it was also unusually smooth. Speed fluctuations were small between DoY 141 and DoY 153. Comparing this time to the slow wind interval in Figure 6b, the average speeds are the same, but the standard deviation is 31% smaller at quadrature. Referring to the subintervals I1, I2, and I3, the density and temperature were also unusually smooth in intervals I1 and I3. Conversely, they exhibited more typical fluctuations during interval I2. In the corona, interval I2 corresponded to the time when the streamer belt appeared to fan out into a forest of rays in LASCO C2 (Figure 3). The Wilcox Solar Observatory $2.5 R_{\text{SUN}}$ neutral line map (Figure 4) shows a ripple or bump in the neutral line at about the same location as the forest, and there was a north-south trending region of more complex field structure in the photosphere, beneath the

forest. It is our interpretation that the forest represents a view across an inclined portion of the streamer belt at this time, a situation and interpretation which are identical to those suggested by Wang *et al.* [1997] for a period during 1996. We note in passing that the forest of rays in LASCO was also visible in UVCS Ly α intensity, a density proxy, although we do not show intensity versus latitude here. The related density fluctuations at Ulysses could either be the ray-like structures in the corona being swept past the Ulysses foot point by solar rotation or, alternatively, a series of small transients embedded in the tilted streamer. However, no evidence of such a group of small transients was seen in LASCO.

Considering UVCS data from the quadrature, there may be an indication of larger Doppler dimming at a height of $4.5 R_{\text{SUN}}$ than at $3.5 R_{\text{SUN}}$, where the oxygen speed is presumably well below 100 km s^{-1} (see section 4). This suggests flow speeds of $< 100 \text{ km s}^{-1}$ at $3.5 R_{\text{SUN}}$.

If it is assumed that the bright streamer boundary is the fast/slow solar wind boundary, then this boundary must not have moved significantly equatorward between a few solar radii and 5 AU. Specifically, the boundary of the coronal hole flow could not have moved equatorward by more than a few degrees. This is simply because there was no hint of fast solar wind at Ulysses. Also, there is no evidence of mixing due to shear instabilities on the interface between slow and fast wind [Siregar *et al.*, 1993] at Ulysses such as would be indicated by episodic appearance of fast solar wind or oscillations in the magnetic field and bulk flow. This is true across all three intervals I1, I2, and I3.

3. CMEs

The activity throughout the quadrature observing interval, as deduced from LASCO C2 movies and individual images, is summarized in Table 1. In that table it is indicated that there were small CMEs on May 23 (DoY 142) and May 25 (DoY 144), and again on June 1 (DoY 152). The CMEs on May 23 and 25 are shown in Figure 11. There is no counterpart to the CMEs on May 23 and June 1 in the data shown in Figures 7 and 8, so these CMEs were probably located off the limb and moving in an unfavorable direction. The C2 images in Figure 11 support this, showing that the CMEs overlie the streamers, and Table 1 notes that the streamer belt appeared unaffected by the passage of the CMEs. Therefore it is likely that these CMEs were erupting magnetic structures either in front of or behind the visible disk and not directly above the east limb.

Conversely, the small shock on DoY 144 (Figure 7) is coincident with the CME on May 25. This raises the question of whether that CME might have been the source of this small shock and/or the fluctuations in temperature, density, and field strength observed in interval I2.

There are several interplanetary manifestations of CMEs that are discussed in the literature. Some of

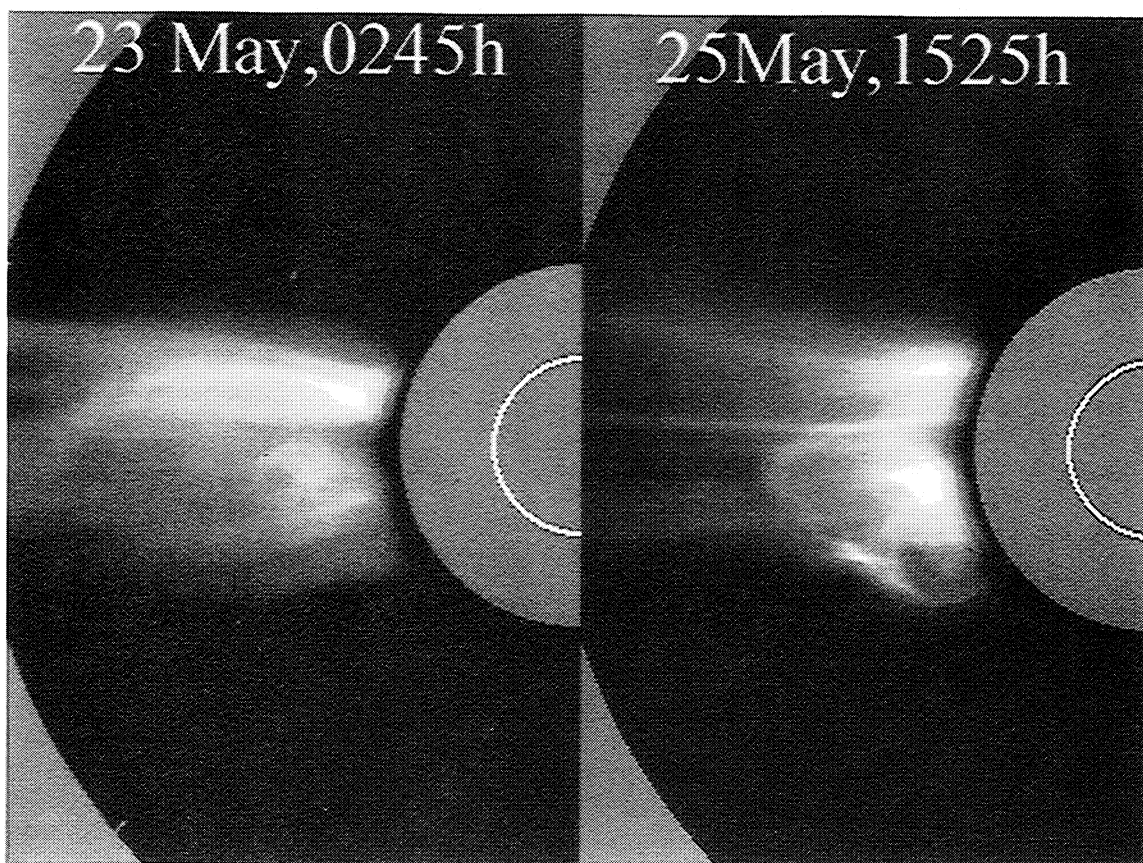


Figure 11. C2 images of the CMEs observed on May 23 and 25, 1997.

these relate to those CMEs which result in magnetic clouds. A magnetic cloud is associated with a rotation in the interplanetary magnetic field [Klein and Burlaga, 1982] which is thought to indicate the presence of a magnetic flux rope that is the signature of the filament that existed at the origin point of the cloud on the Sun. We plot the meridional and azimuthal components of the IMF in Figure 12 (in Sun-centered heliographic polar coordinates), and it is obvious that there is a partial rotation of the IMF in the B_ϕ component during interval I2. The field begins turning eastward on DoY 145, is furthest east on DoY 147, and returns to the radial direction on DoY 151, so that the total duration of the eastward turning is almost a week. Typically, clouds last a day or so at 1 AU, and expand with increasing heliocentric distance, so this duration is not inconsistent with the model. Furthermore, it is fairly common for a magnetic cloud to drive a shock in front of it and this rotation corresponds to the low ion plasma β interval noted in Figure 6a. However, the flow vector components suggest that this may not be a cloud at all. The velocity components V_θ and V_ϕ are plotted at the bottom of Figure 12. V_ϕ turns westward at the shock and then rotates to the east. This is a typical CIR signature. V_θ turns strongly southward at the shock and rotates back to the radial direction, which is

unusual for a magnetic cloud but is typical for a flow being driven by a nearby CIR [e.g. Pizzo and Gosling, 1994]. The low helium abundance in the shaded area of Figure 6a, noted earlier, is also typical of CIRs [Borrini *et al.*, 1981, Figure 4].

To investigate further whether the eastward B_ϕ shown in Figure 12 might have been a magnetic cloud, we also looked for bidirectional streaming of energetic electrons, a reliable signature of the presence of locally closed magnetic field lines since the electrons will tend to circulate in both directions along the field [Gosling *et al.*, 1987]. No bidirectional streaming was visible in 84-115 eV electrons (those corresponding to coronal temperatures) on June 19, 20, and 21 (DoY 170, 171, and 172 in Figure 6). On June 18 (DoY 169), the day after the small shock, there was some weak counterstreaming but no significant evidence of a magnetic cloud. Typically, for a magnetic cloud strong bidirectional streaming would begin with the eastward turning of the field and persist for anywhere from half to the full duration of the cloud. Therefore, we suspect that the weak events observed on 18 June do not show the presence of a magnetic cloud.

The Fe XIV north polar coronal hole boundaries from CR1922 and CR1923 are plotted in Figure 5. This shows that the polar coronal hole that drove the high speed streams in earlier rotations (shown in Figure 2b)

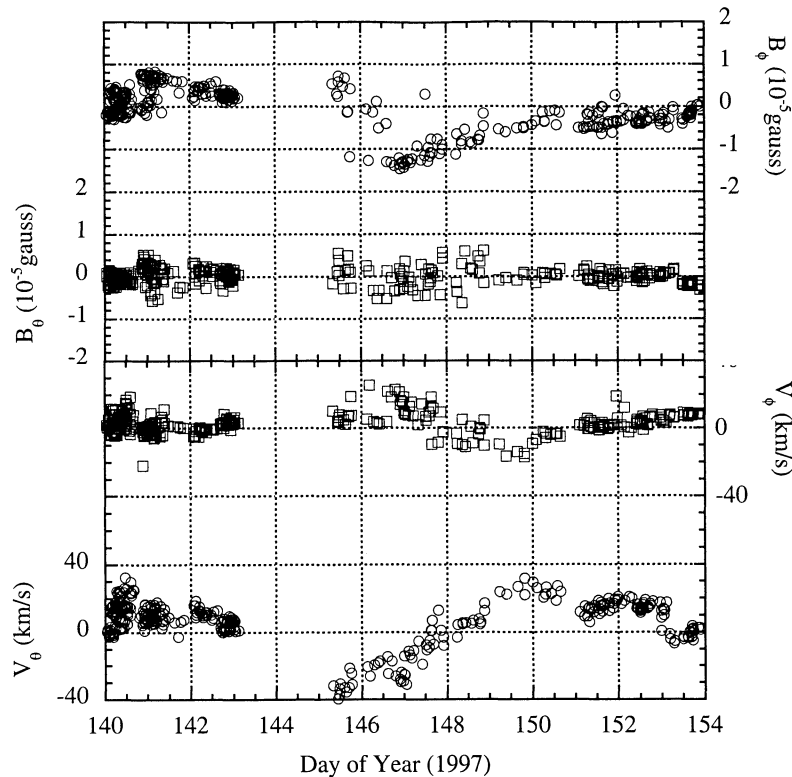


Figure 12. Hourly average values of the interplanetary magnetic field vector and solar wind velocity meridional and azimuthal components (in Sun-centered heliographic coordinates) at Ulysses, as mapped back to the origin time at the Sun (see Figure 7). In the top plot, circles denote B_ϕ and squares denote B_θ . In the bottom panel, squares denote V_ϕ and circles denote V_θ .

has receded by CR 1923 and no high-speed stream was seen at Ulysses during the preceding CR. Moreover, the plots of V_θ , V_ϕ , and B_θ from CR1922 look exactly like those shown in Figure 12, and the Fe XIV map shows the north polar coronal hole still extending toward the equator in CR 1922, between longitudes 0° and 160° . Thus it appears that the eastward turning of the IMF was due to a high-speed stream to the west and north of the Ulysses foot point shown in Figure 4.

From this we conclude that the small shock on DoY 168 in Figure 6 was associated with a CIR north of Ulysses and driven by an equatorial extension of the polar coronal hole that was the last vestige of the large extension which produced the long series of CIRs shown in Figure 2b.

4. A UVCS Transient Event on May 26

Since Ulysses was immersed in exceptionally smooth slow solar wind throughout the quadrature interval, this presents an unusual opportunity to examine more closely a small transient observed by LASCO C2 and possibly identify the same transient at Ulysses. These transients are common but far too small to be classified as CMEs. One such transient, shown in Figure 13, was observed on May 26 at the latitude of Ulysses. In sec-

tion 2 we concluded that the plasma at 10°N moved very little in latitude between the outer edge of the field of view of LASCO C2 and Ulysses at 5 AU at this time, so it is possible this small event could have been detected at Ulysses.

The event, as described above, shows up as a high $I_{Ly\ \alpha}$ data point at $3.5 R_{SUN}$ in Figure 9 on DoY 146 (boxed data point). In Figure 14 (top plot) we show the temporal profile of the Ly α line intensity at $3.5 R_{SUN}$, with a time resolution of the order of 15 min, and (middle plot) the temporal profile of the Ly α line intensity at $4.5 R_{SUN}$, with a time resolution of the order of 20-30 min. The figure refers to observations made over the time interval from DoY 146.66 to 146.98: Unfortunately, between 146.98 and 147.71, we have only a single 5 min observation, which is too short to be of any use. The bottom plot gives the ratio of the OVI 1032 to OVI 1036 line intensities, at 3.5 (pluses) and at 4.5 (crosses) R_{SUN} , averaged over each observing interval.

The enhanced Ly α intensity in the time interval between DoY 146.95 and DoY 146.98 points to a density increase whose maximum must have occurred at the time we were observing at $4.5 R_{SUN}$, possibly associated with the LASCO C2 transient. A density larger than unperturbed densities by a factor ≈ 1.4 accounts

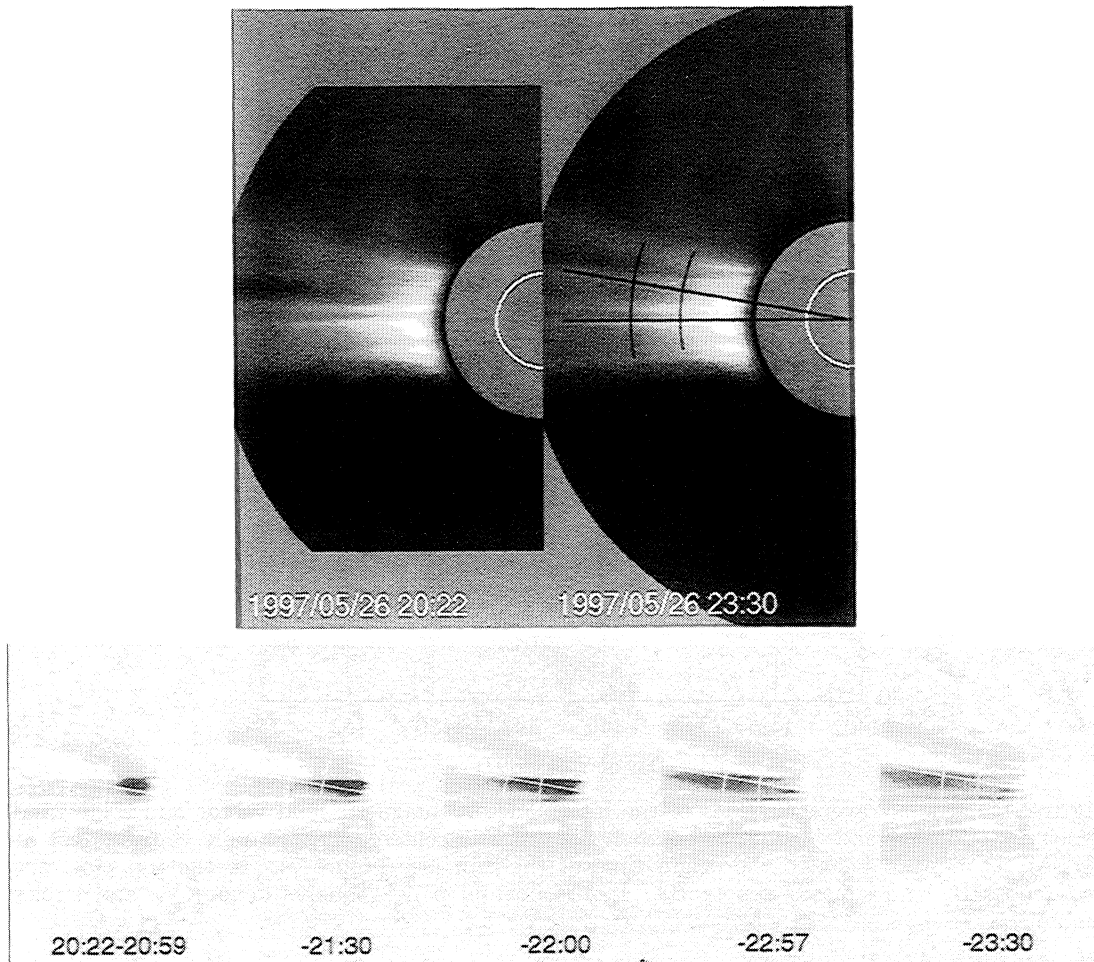


Figure 13. The small transient on May 26. (top) “Before” and “after” images. (bottom) The transient itself is shown in a series of difference images, differenced with respect to the initial image at 2022 and plotted as negatives so that density excess is dark and density deficit is light. The dashed line, being crossed by the dark transient, points toward Ulysses. The fiducial marks on the top right image at 2330 show the heliographic equator, the latitude of Ulysses (10° north of the equator), and the UVCS observing heights of 3.5 and $4.5 R_{SUN}$.

for the observed Ly α variation, and this is a lower limit to the true density enhancement because it was derived assuming Doppler dimming has not affected the data. In the following, we try to give a quantitative estimate of densities, prior to and during this event, under the assumption that prior to the transient the plasma flow speed, both at 3.5 and $4.5 R_{SUN}$, is negligible.

To this end, we need to complement observations at 3.5 and $4.5 R_{SUN}$ with data taken by the standard daily UVCS synoptic program. In the UVCS synoptic program, radial scans are made at six heliocentric heights (from 1.5 up to 2.25 or $3 R_{SUN}$, depending on the observing latitude), moving the slit around the disk in steps of 45° , thus providing radial profiles of the Ly α and OVI line intensities over the entire corona. Identifying the OVI line intensities along the radial direction where the Ulysses-SOHO observations were made, we get the OVI intensity profile from 1.5 to $4.5 R_{SUN}$ (ignoring possible temporal variations between the synop-

tic and the Ulysses-SOHO observations) in the direction pointing to the Ulysses spacecraft. The OVI intensities versus heliocentric distance data allow us to derive the electron density profile over that altitude range: We refer the reader to Corti *et al.* [1997] for a description of the technique we use to this purpose. Here, it suffices to mention that OVI lines have a radiative and a collisional contribution, and that the collisional contribution depends (among other factors) on the square of the electron density, integrated along the line of sight. Identifying the collisional contribution of the 1037 \AA line, and assuming a priori a power law profile for the density versus heliocentric distance, electron densities can be evaluated.

Figure 15 shows the electron density profile for DoY 146 before the transient was observed: Density values agree with those derived (from Van de Hulst inversion of pB data) for the west limb streamers observed in August 1996 by Gibson *et al.* [1999] and are typical

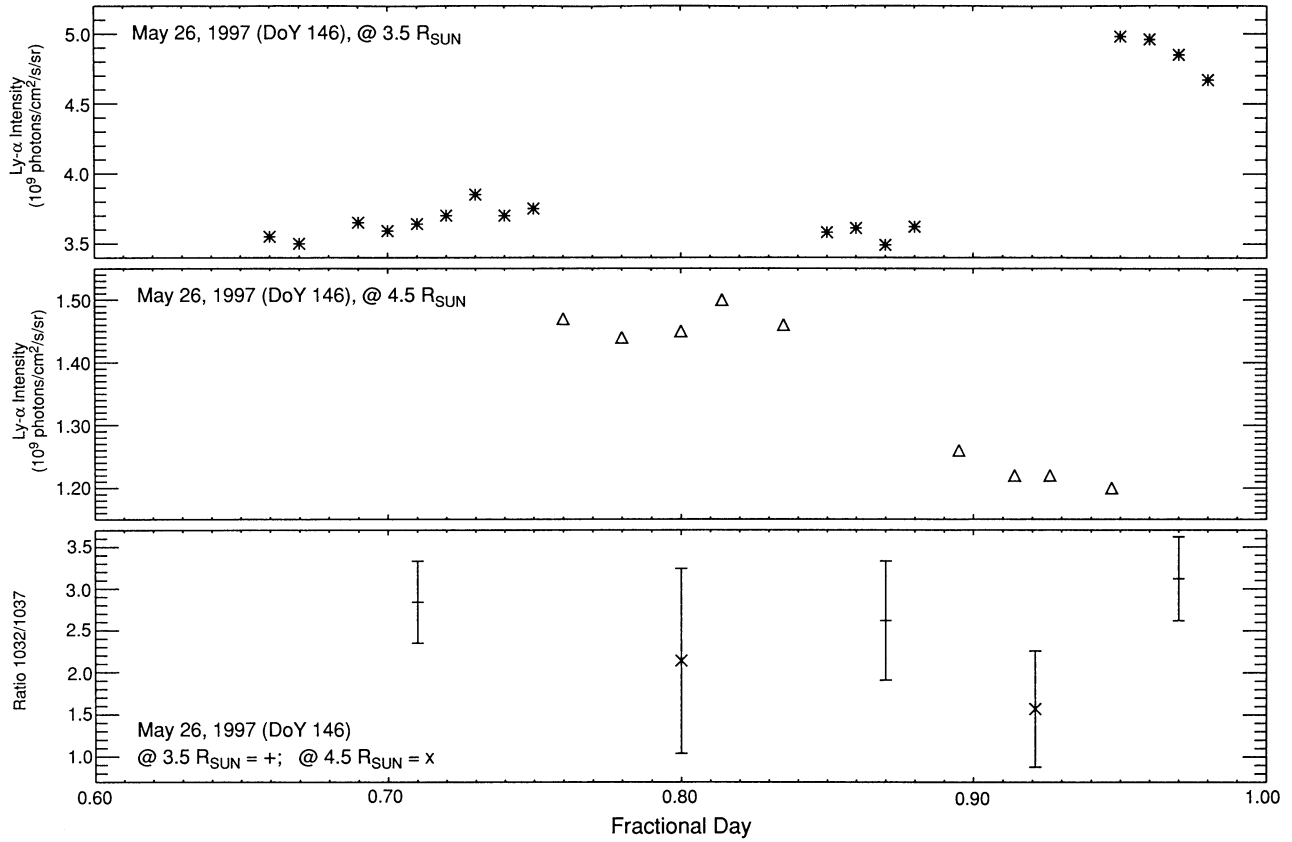


Figure 14. (top and middle) $I_{\text{Ly } \alpha}$ on DoY 146 (May 26) at 3.5 and 4.5 R_{SUN} . Data have a temporal resolution of about 15 min. (bottom) Ratio of 1032/1037 Å line intensities at 3.5 (pluses) and 4.5 (crosses) R_{SUN} . The five data points represent average R values over, respectively, 8100, 7800, 3000, 5700, and 3000 second observing intervals.

of the minimum equatorial corona [Allen, 1962]. This also agrees with the densities derived from LASCO C2 pB analysis for the same locations in the corona to within the size of the error bars shown in Figure 15 (D. Biesecker, private communication, 1999). We will refer to this density profile as the unperturbed density profile, because it has been derived from observations taken prior to the transient event.

Knowledge of the unperturbed electron density versus height profile allows us to check whether the unperturbed Ly α intensities at 3.5 and 4.5 R_{SUN} can be reproduced by a steady plasma. In this case we may move on and evaluate the plasma flow speed and density during the transient event. We remind the reader that the total (i.e., integrated over the line profile) Ly α intensity, as observed along the line-of-sight (LOS) direction \mathbf{n} is given by

$$I_{\text{Ly}-\alpha} = \frac{hB_{12}\lambda_0}{4\pi} \int_{-\infty}^{\infty} N_1 dx \int_{\Omega} p(\varphi) F(\delta\lambda) d\omega' \quad (1)$$

where h is the Planck constant; B_{12} is the Einstein coefficient for the line; λ_0 is the rest value for the central wavelength λ of the Ly α transition; N_1 is the number density of hydrogen atoms in the ground level; the unit

vector \mathbf{n} is along the line of sight x and the unit vector \mathbf{n}' is along the direction of the incident radiation; φ is the angle between \mathbf{n} and \mathbf{n}' ; $p(\varphi) d\omega'$ (where ω' is the solid angle around \mathbf{n}') is the probability that a photon traveling along the direction \mathbf{n} was traveling, before scattering, along the direction \mathbf{n}' ; Ω is the solid angle subtended by the chromosphere at the point of scattering; $\delta\lambda$ is the red shift; I_{chrom} is the exciting chromospheric radiation and Φ is the coronal absorption profile. For the sake of simplicity, in the following, we assume that the whole Ly α emission comes, at 3.5 and 4.5 R_{SUN} , from a steady plasma at uniform temperature and density, which extends along the LOS over a length L . The parameter L is estimated from the observations taken at 3.5 R_{SUN} and used to evaluate the $I_{\text{Ly } \alpha}$ at 4.5 R_{SUN} , to check on the consistency of this simplified scenario.

If the Ly α line originates from a slab at constant temperature and density, with no plasma flow, its intensity is given by

$$I_{\text{Ly}-\alpha} \approx (\text{const}) f(T_e) F(T_k) N_e L, \quad (2)$$

where the kinetic temperature T_k is constrained by the width of the line and T_e is the electron temperature.

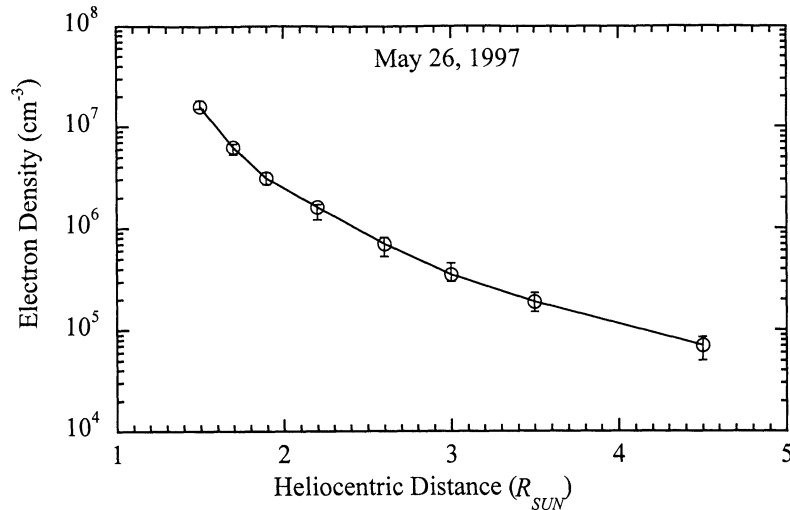


Figure 15. Electron density versus heliocentric distance along the Sun-Ulysses radius for May 26, 1997. Error bars are derived from uncertainties in the parameters given by the best fitting technique used to derive N_e values (see text).

The kinetic temperature T_k is rather well known in streamers; see, for example, *Kohl et al.* [1997], *Miralles et al.* [1999], and *Maccari et al.* [1999]. In the following we will assume $T_k = 1.6 \times 10^6$ K, in agreement with results from the previous authors. We note that T_k values in the literature refer to temperatures perpendicular to the magnetic field; parallel kinetic temperatures are essentially unknown, and their values are generally chosen in between electron and perpendicular temperature values. We assume $T_{\parallel} = 1.2 \times 10^6$ K for Ly α : Changing the value of T_{\parallel} from $T_{\parallel} = T_e$ to $T_{\parallel} = T_k$ changes the Ly α intensity by no more than 15%. There are a few electron temperature evaluations in streamers, at low altitudes (see, for example, *Raymond et al.* [1997], *Li et al.* [1998], *Frazin et al.* [1999], and *Parenti et al.* [1999]), but the only estimate at higher levels has been made by *Fineschi et al.* [1998], who gave a value of $T_e = 1.1 \times 10^6 \pm 0.25 \times 10^6$ K at $2.7 R_{\text{SUN}}$. In the following, we will assume $T_e = 10^6$ at $3.5 R_{\text{SUN}}$, and $T_e = 0.9 \times 10^5$ K at $4.5 R_{\text{SUN}}$, on the grounds that T_e is likely to slowly decrease as we move outward from the Sun. The choice of T_e is not crucial: The neutral hydrogen abundance varies by $< 10\%$, when T_e changes from 1.1 to 1×10^6 K, and by 20% , when T_e changes from 10^6 to 9×10^5 K.

The observed intensity of the Ly α line at $3.5 R_{\text{SUN}}$ is reproduced with the choice of T_k , T_{\parallel} , and T_e mentioned above and the N_e value given at that altitude by the unperturbed density profile, provided the integration length is on the order of 2 solar radii. Assuming a radial expansion of the emitting region, densities from the unperturbed profile, and temperatures mentioned above, we reproduce the Ly α intensity at $4.5 R_{\text{SUN}}$ fairly well ($I_{\text{Ly } \alpha} = 1.3 \times 10^9$ ph cm $^{-2}$ s $^{-1}$ sr $^{-1}$ versus an observed value of $\approx 1.45 \times 10^9$ ph cm $^{-2}$ s $^{-1}$ sr $^{-1}$).

We conclude that order of magnitude estimates of $I_{\text{Ly } \alpha}$, at 3.5 and $4.5 R_{\text{SUN}}$ are consistent with the hypothesis that at those levels, plasma flow speeds are negligible.

Further support for this scenario comes from OVI lines: The observed OVI line intensities, and ratio, are consistent with values we obtain by calculating the OVI line intensities with the density, integration length and electron temperature used for Ly α . At $3.5 R_{\text{SUN}}$, the OVI kinetic temperature has been taken to be $T_k = 1.4 \times 10^7$ K, from estimates given by *Kohl et al.* [1997] and *Frazin et al.* [1999], and we assumed $T_{\parallel} = 3 \times 10^6$ K. With these physical parameters we get line intensities which agree with observations (e.g., $I_{\text{OVI},1037} = 1.1 \times 10^7$ ph cm $^{-2}$ s $^{-1}$ sr $^{-1}$, precisely as observed). It is worth noting that a ratio R of the OVI 1032 to OVI 1037 line intensities of the order of 2.9-3.1 is compatible with flow speed lower than 50 km s $^{-1}$. Such flow speeds would leave the Ly α intensity practically unaffected (variations lower than 5%) and relax somewhat our previous assumption of a steady plasma. The presence of flows of this order of magnitude is confirmed by the evaluation of the OVI line intensities at $4.5 R_{\text{SUN}}$, where the best agreement with observations (values within the error bar of measured intensities, which are of the order of 30%, or larger) is obtained by assuming an outflow of 40 km s $^{-1}$. This is comparable to the lowest speeds reported by *Sheeley et al.* [1997] at $4.5 R_{\text{SUN}}$ using time-lapse sequences of LASCO images.

Once the unperturbed physical parameters have been determined, we may examine the transient event. At the time of the UVCS transient, at DoY ≈ 146.95 , at $3.5 R_{\text{SUN}}$, the Ly α intensity increases by a factor of 1.4, implying densities of about 3×10^5 cm $^{-3}$ (this is a lower limit to the actual density increase, as we assume

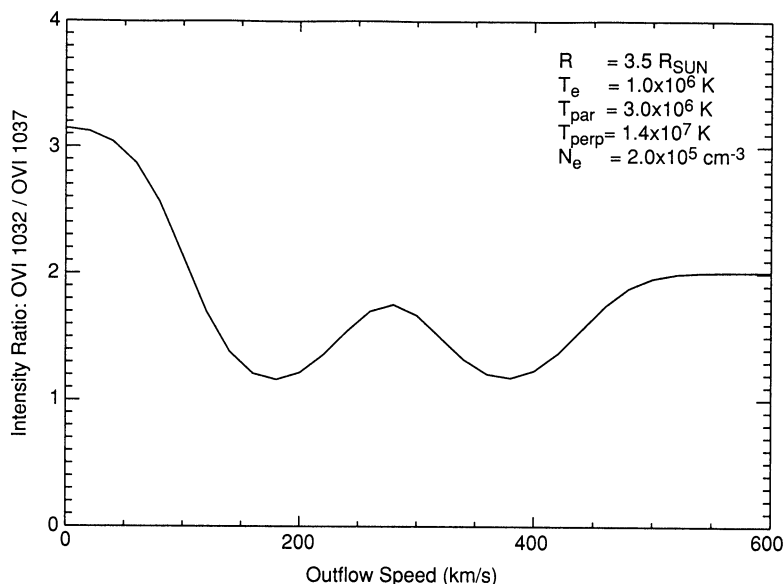


Figure 16. Profile of the ratio R of the total intensity of OVI 1032 Å to OVI 1037 Å lines as a function of the plasma outflow speed, for the set of parameters given in the figure.

that no dimming is present). At $4.5 R_{\text{SUN}}$, if we allow for the same density increase and in the absence of appreciable plasma flows, we would expect an analogous increase of the Ly α intensity. On the contrary, the Ly α intensity drops by about 20%. This allows us to make an estimate of the differential flow speed, between 3.5 and $4.5 R_{\text{SUN}}$, necessary to account for the observed low intensity value, from a Doppler dimming calculation. It turns out that the plasma flow speed is of the order of 125 km/s. This is consistent with the 100 km s $^{-1}$ derived from inspection of the westward motion of the event in Figure 13.

At this flow speed, the OVI lines are strongly dimmed, and the ratio between the 1032 and 1037 Å line intensities is shown by Figure 16 to be $R = 1.45$. Although the error bar in the “observed” R value, at $4.5 R_{\text{SUN}}$, is so large that any value between 0.9 and 2.2 is acceptable, predicted and observed values agree fairly well. What is perhaps even more significant is that the only time when it is impossible to find a unique value of R , fitting within the error bars of the observed values at 3.5 and $4.5 R_{\text{SUN}}$, is the time interval under examination, for which a substantial flow speed has been inferred, and a minimum value of R is found.

The event we observed turned out to have a minimal density increase, with respect to the unperturbed situation, of a factor of 1.4, and a speed of the order of 125 km s $^{-1}$. As we pointed out, this is not a unique interpretation, although it is consistent with all our data. For instance, we cannot rule out larger outflow speeds, at $3.5 R_{\text{SUN}}$, if data at DoY 146.95 were affected by Doppler dimming that goes unrevealed. In passing, we notice that the range of altitudes where we observed,

and the outflow speed we derived, is the same range where Wang *et al.* [1998], from LASCO data, observed the birth of plasma “blobs” at the top of helmet streamers flowing outward with initial speed of the same order of magnitude as the outflow that we evaluated. The event we examined is more like a small CME, but the speed is like the blobs.

We now address briefly the other case when UVCS observations show an anomalous data point. The only time when R gives an indication of a high outflow at $3.5 R_{\text{SUN}}$ is on May 23, in the time interval between 1932 and 2017 UT, when $R = 1.2$. It is unfortunate that the values of R at the higher heliocentric distance are so uncertain (the errors are of the order 100%) that we do not have any reliable indication of the plasma conditions at that level. Quite likely, the presence of such high uncertainty points to a weakening of the lines, and hence to the persistence of high flows also beyond $3.5 R_{\text{SUN}}$. The Ly α intensity, on the other hand, though brighter by nearly 50% than it was on the previous day, shows no fluctuations during the observations of May 23. Data do not provide us with sufficient information to understand what caused the low R , high-speed plasma we observe. Seemingly, it was a velocity event, unaccompanied by density variation. The in situ data do not show any anomalously high speed data point, as expected for small-scale speed fluctuations (see section 2.2).

5. Summary

The May 1997 SOHO-Ulysses quadrature presented an extraordinary opportunity for analyzing slow solar wind originating from a solar minimum streamer belt.

Ulysses was only 10° north of the equator, near the latitude of the bright boundary of the streamers lying on the limb at that time, and detected nothing but unusually smooth slow wind. The precise quadrature date was May 26 but owing to the slow orbital motion of SOHO and Ulysses around the Sun, data from up to a week on either side of the quadrature can be assumed to come from the limb, to within the accuracy of the extrapolation between Ulysses and the Sun. During this time the Sun will turn through almost half of a full solar rotation, with different features rotating onto and off of the limb beneath the foot point of Ulysses.

We used LASCO C2 images ($2-6 R_{\text{SUN}}$) to assess the morphology of the features on the limb and three major intervals were identified: I1, I2, and I3. There were simple, isolated streamers on the limb during I1 and I3, but the streamer belt fanned out into a forest of rays during I2. Using Wilcox Solar Observatory photosphere and source surface magnetic field maps, we conclude that I2 resulted from a region where the streamer belt was inclined to the heliographic equator and hence was being viewed obliquely. This is a situation very similar to that reported by Wang *et al.* [1997], where they diagnosed conditions using a model and synthetic images that closely reproduced the observations.

An important result is that throughout the quadrature interval, Ulysses was very close to the extrapolated latitude of the bright boundary of the streamer belt, sometimes within only a degree or two of its latitude. Nevertheless, no evidence was seen of any fast solar wind or of any mixing between fast and slow solar wind. If it is assumed that the brightness boundary and the fast/slow wind boundary are the same, then there could have been no significant further equatorward motion of that boundary between $6 R_{\text{SUN}}$ and 5.1 AU. In addition, there is no evidence of the presence of shear instabilities on the interface between fast and slow wind.

Three small CMEs were observed in LASCO C2 during the quadrature interval. These CMEs generally appeared to leave the streamer belt on the limb unaffected and it was concluded that they all originated from regions sufficiently far off the limb that any resulting interplanetary disturbances completely missed Ulysses. The small shock visible on DoY 168 in Figure 6 was probably due to a CIR lying north of the latitude of Ulysses. The CIR-induced shock would have originated somewhere inside 5 AU and propagated equatorward to the latitude of Ulysses. The equatorward flow following the shock is insufficient to move the streamer boundary equatorward by more than $\sim 2^\circ$. The low ion plasma β region identified in Figure 6a has some properties of CMEs but is more likely due to some inherent property of slow wind coming from the inclined streamer belt.

The extraordinarily quiet conditions during the quadrature interval offered the opportunity of more closely examining small transients observed in white light in LASCO C2 and in spectral emission with UVCS. Such comparisons have not been made before between SOHO

and Ulysses. The two transients which we examined have a signature in the plasma outflow speed, as seen from UVCS 1032/1037 OVI line ratio, which is apparently higher than in standard conditions. The signature, however, is completely lost at the distance of Ulysses, as expected. UVCS data show that in one of the events (May 26) there is a density increase which is possibly identifiable in in situ data as the density spike on DoY 147.5 in Figure 7 (solid data points). Analysis of the UVCS transient allowed us to derive average plasma parameters (density, temperature, and outflow speed) close to the Sun: Its main characteristics can be reproduced by assuming that only density changed, with respect to preevent conditions. This compares well with Ulysses data, where a density increase unaccompanied by any variation in temperature and flow speed has been observed in association with the LASCO/UVCS transient. We conclude that with the exception of flow speeds, plasma variability at low coronal heights can be reliably transported to the far distant solar wind plasma under quiet conditions that prevailed during this time. This is the first time such a comparison has been attempted, and we will need to analyze additional quadratures to lend general support to our conclusions.

Acknowledgments. The work of G.P. was partially supported by the Italian Space Agency (ASI). The work of S.S. was supported by the SWOOPS and UVCS experiment teams and by ASI. The work of M.N. and B.G., was carried out at the Jet Propulsion Laboratory, California Institute of Technology, under contract with the National Aeronautics and Space Administration. We thank the Ulysses VHM/FGM experiment team (A. Balogh, PI) for use of their magnetometer data and the Yohoh SXT experiment team for use of their X-ray coronal images. SOHO and Ulysses are missions of international cooperation between ESA and NASA.

Janet G. Luhmann thanks Herbert O. Funsten and Neil R. Sheeley Jr. for their assistance in evaluating this paper.

References

- Allen, C. W., *Astrophysical Quantities*, 2nd ed., Athlone, London, 1962.
- Borriani, G., J. T. Gosling, S. J. Bame, W. C. Feldman, and J. M. Wilcox, Solar wind helium and hydrogen structure near the heliospheric current sheet: A signal of coronal streamers at 1 AU, *J. Geophys. Res.*, **86**, 4565, 1981.
- Brueckner, G. E., et al., The large angle spectroscopic coronagraph (LASCO), *Sol. Phys.*, **162**, 357, 1995.
- Corti, G., G. Poletto, M. Romoli, J. Michels, J. L. Kohl, and G. Noci, Physical parameters in plume and interplume regions from UVCS observations, in *The Corona and the Solar Wind Near Minimum Activity*, Eur. Space Agency Spec. Publ., ESA-SP404, 289, 1997.
- Cranmer, S. R., et al., An empirical model of a polar coronal hole at solar minimum, *Astrophys. J.*, **511**, 481, 1999.
- Fineschi, S., L. D. Gardner, J. L. Kohl, M. Romoli, and G. Noci, Grating stray light analysis and control in the UVCS/SOHO, *Proc. SPIE Int. Soc. Opt. Eng.*, **3443**, 67, 1998.
- Frazin, R.A., A. Ciaravella, E. Dennis, S. Fineschi, L. D. Gardner, J. Michels, R. O'Neal, J. C. Raymond, C.-R.

- Wu, J. L. Kohl, A. Modigliani, and G. Noci, UVCS/SOHO ion kinetics in coronal streamers, *Space Sci. Rev.*, **87**, 189, 1999.
- Gardner, L. D., et al., Stray light, radiometric, and spectral characteristics of UVCS/SOHO: Laboratory calibration and flight performance, *Proc. SPIE Int. Soc. Opt. Eng.*, **2831**, 2, 1996.
- Gibson, S. E., A. Fludra, F. Bagenal, D. Biesecker, G. Del Zanna, and B. Bromage, Solar Minimum streamer densities and temperatures using Whole Sun Month coordinated data sets, *J. Geophys. Res.*, **104**, 9691, 1999.
- Gosling, J. T., D. N. Baker, S. J. Bame, W. C. Feldman, R. D. Zwickl, and E. J. Smith, Bidirectional solar wind electron heat flux events, *J. Geophys. Res.*, **92**, 8519, 1987.
- Klein, L. W., and L. F. Burlaga, Interplanetary magnetic clouds, *J. Geophys. Res.*, **87**, 613, 1982.
- Kohl, J. L., and G. L. Withbroe, EUV spectroscopic plasma diagnostics for the solar wind acceleration region, *Astrophys. J.*, **256**, 263, 1982.
- Kohl, J. L., et al., First results from the SOHO Ultraviolet Coronagraph Spectrometer, *Sol. Phys.*, **175**, 613, 1997.
- Li, J., J. C. Raymond, L. W. Acton, J. L. Kohl, M. Romoli, G. Noci, and G. Naletto, Physical structure of a coronal streamer in the closed-field region as observed from UVCS/SOHO and SXT/Yohkoh, *Astrophys. J.*, **506**, 431, 1998.
- Maccari, L., G. Noci, S. Fineschi, A. Modigliani, M. Romoli, and J. L. Kohl, Ly- α observation of a coronal streamer with UVCS/SOHO, *Space Sci. Rev.*, **87**, 265, 1999.
- McComas, D. J., et al., Ulysses' return to the slow solar wind, *Geophys. Res. Lett.*, **25**, 1, 1998.
- Miralles, M. P., L. Strachan, L. D. Gardner, P. Smith, J. L. Kohl, M. Guhathakurta, and R. R. Fisher, Properties of coronal hole-streamer boundaries and adjacent regions as observed by Spartan 201, *Space Sci. Rev.*, **87**, 277, 1999.
- Neugebauer, M., B. E. Goldstein, D. J. McComas, S. T. Suess, and A. Balogh, Ulysses observations of microstreams in the solar wind from coronal holes, *J. Geophys. Res.*, **100**, 23,389, 1995.
- Noci, G., J. L. Kohl, and G. L. Withbroe, Solar wind diagnostics from Doppler-enhanced scattering, *Astrophys. J.*, **315**, 706, 1987.
- Parenti, S., G. Poletto, J. C. Raymond, and B. J. I. Bromage, Physical conditions in a high latitude streamer from CDS and UVCS observations, in *Plasma Dynamics and Diagnostics in the Solar Transition Region and Corona*, *Eur. Space Agency Spec. Publ.*, **ESA-SP446**, 541, 1999.
- Phillips, J. R., et al., Ulysses solar wind plasma observations from pole to pole, *Geophys. Res. Lett.*, **22**, 3301, 1995.
- Pizzo, V. J., and J. T. Gosling, 3-D simulation of high-latitude interaction regions: Comparison with Ulysses results, *Geophys. Res. Lett.*, **21**, 2063, 1994.
- Raymond, J. C., et al., Composition of coronal streamers from the SOHO Ultraviolet Coronagraph Spectrometer, *Sol. Phys.*, **175**, 645, 1997.
- Sheeley, N. R., Jr., et al., Measurements of flow speeds in the corona between 2 and 30 R_{\odot} , *Astrophys. J.*, **484**, 472, 1997.
- Siregar, E., D. A. Roberts, and M. L. Goldstein, Quasi-periodic transverse plasma flow associated with an evolving MHD vortex street in the outer heliosphere, *J. Geophys. Res.*, **98**, 13,233, 1993.
- Suess, S. T., G. Poletto, G. Corti, G. Simnett, G. Noci, M. Romoli, J. Kohl, and B. E. Goldstein, Ulysses-UVCS coordinated observations, *Space Sci. Rev.*, **87**, 319-322, 1999.
- Wang, Y.-M., et al., Origin and evolution of coronal streamer structure during the 1996 minimum activity phase, *Astrophys. J.*, **485**, 875, 1997.
- Wang, Y.-M., N. R. Sheeley, Jr., J. H. Walters, G. E. Brueckner, R. A. Howard, D. J. Michels, P. L. Lamy, R. Schwenn, and G. M. Simnett, Origin of streamer material in the outer corona, *Astrophys. J.*, **498**, L165, 1998.
- Weber, E. J., and L. Davis, Jr., The angular momentum of the solar wind, *Astrophys. J.*, **148**, 217, 1967.
- Withbroe, G. L., J. L. Kohl, H. Weiser, and R. H. Munro, Probing the solar wind acceleration region using spectroscopic techniques, *Space Sci. Rev.*, **33**, 17, 1982.

B. E. Goldstein and M. Neugebauer, Jet Propulsion Laboratory, MS 169-506, 4800 Oak Grove Drive, Pasadena, CA 91109.

G. Poletto, Osservatorio Astrofisico di Arcetri, Largo Enrico Fermi, 5, 50125 Firenze, Italy.

M. Romoli, Department of Astronomy, Università di Firenze, I-50125 Firenze, Italy.

G. M. Simnett, Department of Space Research, School of Physics and Astronomy, University of Birmingham, Birmingham B15 2TT, England, United Kingdom.

S. T. Suess, NASA Marshall Space Flight Center, MS SD50, Huntsville, AL 35812. (steve.suess@msfc.nasa.gov)

(Received February 14, 2000; revised April 21, 2000; accepted April 21, 2000.)